Chlamydophila pneumoniae attachment and infection in low proteoglycan expressing human lymphoid Jurkat cells

Miho Kobayashi[1,5], Kasumi Ishida[1], Junji Matsuo[1], Shinji Nakamura[2], Ayumi Nagasawa[1], Kazuki Motohashi[1], Takashi Yao[3], Itaru Hirai[4], Yoshimasa Yamamoto[4], Haruki Suzuki[5], Chikara Shimizu[5], Kazuhiko Matsuno[1,5]

Hiroyuki Yamaguchi[1]*

[1]*Department of Medical Laboratory Sciences, Faculty of Health Sciences, Hokkaido University, Nishi-5 Kita-12 Jo, Kita-ku, Sapporo, Hokkaido 060-0812, Japan*

[2]*Division of Biomedical Imaging Research, Juntendo University Graduate School of Medicine, 2-1-1 Hongo, Bunkyo-ku, Tokyo 113-8421, Japan*

[3]*Department of Pathology (I), Juntendo University School of Medicine, 2-1-1 Hongo, Bunkyo-ku, Tokyo 113-8421, Japan*

[4]*Laboratory of Molecular Microbiology, Department of Bioinformatics, Graduate School of Medicine, Osaka University, 1-7 Yamadaoka, Suita, Osaka 565-0871, Japan*

[5]*Hokkaido University Hospital, Nishi-5 Kita-14 Jo, Kita-ku, Sapporo, Hokkaido 060-0812, Japan*

*Corresponding author.

Mailing address: Department of Medical Laboratory Sciences, Faculty of Health Sciences, Hokkaido University, Nishi-5 Kita-12 Jo, Kita-ku, Sapporo, Hokkaido 060-0812, Japan

Phone: +81-11-706-3326 / FAX: +81-11-706-3326

E-mail: hiroyuki@med.hokudai.ac.jp

ABSTRACT

This study investigated the proteoglycan (PG)-dependent mechanism of *Chlamydophila pneumoniae* attachment to lymphocytic cells. Lymphoid Jurkat cells and epithelial HEp-2 cells were statically infected with *C. pneumoniae* (TW183). Transmission electron microscopy and assessment of inclusion-forming units indicated that the bacteria grew normally in Jurkat cells and were capable of producing secondary infection; however, they grew at a slower rate than in HEp-2 cells. RT-PCR analysis indicated that HEp-2 cells strongly expressed PG-core protein encoding genes, thereby sustaining glycosaminoglycans (GAGs), such as heparin, on the cellular surface. Similar gene expression levels were not observed in Jurkat cells, with the exception of *glypican-1*. Immunofluorescence analysis also supported strong heparin expression in HEp-2 cells and minimal expression in Jurkat cells, although heparan sulfate pretreatment significantly inhibited bacterial attachment to both cell types. Immunofluorescent co-staining with antibodies against chlamydial LPS and heparin did not identify bacterial and heparin co-localization on Jurkat cells. We also confirmed that when *C. pneumoniae* was statically infected to human $CD4^+$ peripheral blood lymphocytes known not expressing detectable level of heparin, the bacteria attached to and formed inclusion bodies in the cells. Thus, the attachment mechanism of *C. pneumoniae* to Jurkat cells with low PG expression is unique when compared with HEp-2 cells and potentially independent of GAGs such as heparin.

Keywords: *Chlamydophila pneumoniae*; lymphocytes; Jurkat cells; heparin; proteoglycans; glycosaminoglycans

1. Introduction

Chlamydophila pneumoniae is an obligate intracellular bacterium and human respiratory pathogen that causes pneumonia [1-3]. Current studies indicate that this organism may also induce chronic inflammatory diseases such as asthma, arthritis, endocarditis and atherosclerosis [4-7]. Although accumulating studies have indicated a possible link between *C. pneumoniae* infection and chronic inflammatory diseases, the bacterial mechanisms involved in disease development remain unclear [8]. In addition to macrophages, lymphocytes are the major immune cell associated with the development of chronic inflammatory diseases, such as atherosclerosis [9, 10]. Therefore, possible direct interactions between lymphocytes and *C. pneumoniae* may contribute to the pathogenesis of chronic inflammatory diseases.

C. pneumoniae, like all other chlamydiae, has an unique developmental cycle that is not present in any other bacterial families and is characterized by two functionally and morphologically distinct bacterial forms, the reticulate body (RB) and elementary body (EB) [11-13]. Infection is initiated by the metabolically inactive EB that differentiates into the larger, metabolically active RB after endocytosis [11-13]. Maturation further occurs in the surrounding plasma membrane known as an inclusion [11-13]. Recently, our studies demonstrated that *C. pneumoniae* can infect and multiply in the human lymphocyte cell line Molt-4 and mouse spleen lymphocytes [14, 15]. Furthermore, Kaul *et al*. reported *C. pneumoniae* DNA in peripheral blood leukocytes obtained from cardiology patients [16]. Thus, lymphocytes are a potential host cell for *C. pneumoniae* infection. Immune functions of lymphocytes infected with *C. pneumoniae* may

therefore be altered to produce an inappropriate immune response to stimulation that eventually contributes to disease pathogenesis.

Host cell attachment is critical in the pathogenic cycle of *Chlamydia* or *Chlamydophila* species and the underlying mechanisms involved have been extensively studied over many years using epithelial cells, such as HeLa cells, HEp-2 cells, or McCoy cells [17-20]. Data from these experiments suggest that heparin, which is the most common GAG, covalently attaches to the core proteins of PG expressed on the host cells and critically functions as a receptor against chlamydial adhesions, such as the outer membrane protein, OmcB [21] or stress protein, GroEL1 [22]. However, the mechanism of *C. pneumoniae* attachment to lymphocytes remains unknown. We therefore investigated the PG-dependent attachment mechanism of *C. pneumoniae* to Jurkat cells, a representative of human lymphoid cells.

2. Results

2.1. C. pneumoniae attachment to lymphoid Jurkat cells followed by successful infection

Confirmation that *C. pneumoniae* could attach and grow in Jurkat and HEp-2 cells was provided using electron microscopy and one-step growth curve analysis. The cells were statistically infected with the bacteria and incubated for up to 72 h. As shown in Fig. 1 and Fig. 2, the bacteria grew normally in typical inclusions for both cell types (Fig. 1A and D, Fig. 2A), although bacterial growth speed was reduced in Jurkat cells and the

inclusions formed were relatively small (Fig. 1D). Electron microscopy also indicated firm bacterial attachment to the Jurkat cells with bundle-like fibers (Fig. 1B and C). There was a significant difference between the bacterial attachment rates to both cells; the attachment rate to Jurkat cells was approximately 10-fold less than to HEp-2 cells (Fig. 2B). In addition, to prevent influence of endosytosis, we performed an experiment of attachment rate under the condition at 4°C. However, the attachment rate did not differ from that at either 25°C or 37°C [attachment rates; 8.8% (4°C), 15.6% (room temperature, approximately 25°C), 10.6% (37°C)], indicating that affect of endocytosis on this finding is minimal. Taken together, these findings indicated that *C. pneumoniae* could attach to and successfully infect Jurkat cells, although attachment rate of the bacteria to the cells as statically infected is significantly low as compared with that of HEp-2 cells.

We also performed an experiment with centrifugation for infection, and compared the IFU values between in HEp-2 and Jurkat cells. Interestingly, it was confirmed that there was still a significant difference of bacterial attachment rate between the cells, but with an increase of initial bacterial attachment numbers (Fig. 2C and D). Although it remains why centrifugation enhanced attachment rate of the bacteria to Jurkat cells remains unknown, it is possible that an increase of physical pressure by centrifugation causing non-specific interaction between bacteria and cells is involved in this finding. Meanwhile, the results supported that our statically infected system is an optimal condition to assess specific interaction between bacteria and cells, without influence of non-specific attachment mechanism.

2.2. Effect of GAGs on C. pneumoniae *attachment to Jurkat cells*

To confirm the effect of GAGs (heparan sulfate, condroitin sulfate, hyaluronic acid) on *C. pneumoniae* attachment to Jurkat cells, cells were infected with the bacteria in the presence or absence of GAGs and the number of infected cells was determined using immunofluorescence and flow cytometry. Of the GAGs present during infection, only heparan sulfate competitively inhibited the bacterial infectivity to both cell types (Fig. 3). No inhibitory effect of the other GAGs on the bacterial infectivity was observed in both cell types. The inhibitory effect of heparin on bacterial attachment to Jurkat cells was similar to that observed for HEp-2 cells. This is potentially due to physical competitive inhibition rather than the presence of substantial amounts of GAGs, including heparin, on the Jurkat cells.

2.3. Comparison of PG-core protein related gene expressions regulating GAGs between Jurkat cells and HEp-2 cells.

Cell surface expression of GAGs is strictly regulated by PG-core protein [23, 24]. An absence or decrease in PG-core proteins may therefore reduce the expression of GAGs and potentially cause an insufficient interaction between bacteria and host cells, thereby preventing infection [25]. We therefore compared PG-core protein gene expression between Jurkat cells and HEp-2 cells with or without infection using reverse transcription polymerase chain reaction (RT-PCR). The following PG-core protein encoding target genes for RT-PCR were used: *syndecan-1*, *syndecan-2*, *syndecan-4*, *betaglycan*, *glypican-1*, *CD44*, *thrombomodulin*. Genes were strongly expressed in HEp-2 cells, regardless of infection (Fig. 4). No difference in the expression of PG-core

protein genes was observed between infected cells and uninfected cells, indicating that minimal gene expression modulation occurred in HEp-2 cells as a consequence of infection. Jurkat cells did not express any of the PG-core protein encoding genes, except *glypican-1* (Fig. 4), suggesting that these cells exhibit low expression of GAGs such as heparin compared with HEp-2 cells.

2.4. Heparin expression and co-localization of C. pneumoniae *with heparin on the cell surface*

Conventional immunofluorescence microscopy revealed relatively high heparin expression on HEp-2 cells (Fig. 5A: green). Heparin expression levels differed between cell types with minimal expression observed in Jurkat cells (Fig. 5B). Further comparison of heparin expression and its co-localization with *C. pneumoniae* on the surface of both cell types using confocal microscopy are shown in Fig. 5C and D (green, *C. pneumoniae*; red, heparin). Co-localization (orange) between bacteria and heparin was frequently observed on infected HEp-2 cells and not observed on infected Jurkat cells.

2.5. Chlamydial attachment and inclusion formation into purified primary human CD4$^+$ lymphocytes, not expressing detectable level of heparin

Taken together, the results suggested a possibility that *C. pneumoniae* could attach and enter to Jurkat cells independently of heparin followed by bacterial maturation. To confirm this possibility, whether *C. pneumoniae* could infect to primary human CD4$^+$

lymphocytes not expressing detectable level of heparin [25-29] was assessed. As shown in Fig. 6A (A-1 to A-5) and B, conventional microscopic observation with specific antibody against *C. pneumponiae* LPS revealed that the bacteria successfully formed specific inclusions into the purified human $CD4^+$ lymphocytes, with the infection rate of approximately 10 %. To define the bacterial attachment and entry to primary human $CD4^+$ lymphocytes, we furthermore investigated the *C. pneumoniae* infection to the cells by using confocal laser microscopy. As a result, both the bacterial attachment on the cell surface at immediately after infection and the specific inclusion formation inside the cells at 3 days after infection were confirmed (Fig. 6D and E). The results obtained from the experiment with primary $CD4^+$ lymphocytes were strongly supporting a possible infection mechanism of *C. pneumoniae* to Jurkat cells independently of heparin.

3. Discussion

Previously we reported that *C. pneumoniae* infection in lymphocytes down-regulates CD3 expression, a critical ligand for antigen-presenting cells, or down-regulates CD25 expression, which is also a critical receptor for detecting stimulation [30, 31]. These findings suggest that immune functions of *C. pneumoniae* infected lymphocytes may be altered, resulting in an inappropriate immune response to stimulation that eventually contributes to chlamydiae pathogenesis. Hence, investigating the attachment mechanism of *C. pneumoniae* to human lymphocytes is critical for better understanding the pathogen's role in the complicated disease pathogenesis. The bacterial attachment

mechanism was investigated in Jurkat cells, as these cells are a well-characterized human lymphocyte cell line, have representative traits of primary human lymphocytes [32] and have previously been used to study cellular functions and immune responses.

Our study confirmed that following bacterial attachment, typical inclusions formed that were permissive to bacterial growth, resulting in increased infectious progenies in Jurkat and HEp-2 cells. Although bacteria grew slower in relatively smaller inclusions in infected Jurkat cells when compared with HEp-2 cells, Jurkat cell inclusions still contained RB and differentiated EB, with a potential for secondary infection. Reasons for the slower growth speed and smaller inclusion size remain unknown; however, they may be explained by physical differences between the cell types. For example, the lipid trafficking cycle for lymphocytes, which critically regulates bacterial and inclusion maturation [33, 34], is slower than in epithelial cells, thus preventing rapid bacterial maturation in inclusion bodies.

Furthermore, a significant difference in attachment rate after infection was observed between HEp-2 cells and Jurkat cells, implying that weak *C. pneumoniae* attachment to Jurkat cells occurs and is potentially an accidental event. However, TEM images indicated strong bacterial attachment to the Jurkat cells, suggesting that *C. pneumoniae* attaches to Jurkat cells that poorly express GAG or PG and that addition of GAGs to cultures does not affect bacterial attachment. Of the GAGs, only heparin inhibited bacterial attachment to Jurkat cells. Inhibition was also observed for HEp-2 cells, which are representative of epithelial cells and strongly express heparin, a well-known receptor to *C. pneumoniae* or *Chlamydia trachomatis* (except LGV type), on the cellular

surface [17-22]. Heparin, which forms the majority of GAGs, also plays a critical role in host cells as a receptor for the attachment of the other pathogens such as *Bordetella pertussis* [35], *Hemophilus influenzae* [36] or *Neisseria gonorrhoeae* [37]. Although the inhibitory mechanisms preventing bacterial attachment to Jurkat cells remain unknown, the inhibitory role of heparin is likely to be minimal and potentially associated with the strong static electrical charge of this molecule. Thus, the attachment mechanism of *C. pneumoniae* to Jurkat cells poorly expressing PG is unique compared with HEp-2 cells and is potentially independent of heparin.

PGs consist of protein cores that support one or more covalently attached GAG chains, such as chondroitin sulfate or heparin [23, 24]. Therefore, since our data imply a minimal presence of core proteins in Jurkat cells causing poor bacterial attachment, the gene expression of PG-core proteins was assessed using RT-PCR analysis. *Syndecan-1*, *syndecan-2*, *syndecan-4*, *betaglycan*, *glypican-1*, and *thrombomodulin* are expressed in epithelial and endothelial cells [38, 39], and CD44 is expressed in lymphocytes [39, 40]. Each of these PG-related core proteins was also expressed in HEp-2 cells regardless of bacterial infection, indicating that GAGs including heparin are strongly expressed in these cells, allowing for efficient bacterial attachment to these cells. In contrast, the undetectable expression of the core proteins (although only *glypican-1* expression was seen) in Jurkat cells suggested a lower bacterial attachment rate than in HEp-2 cells.

Reportedly, the major PG of lymphocytes is the CD44 molecule, which is expressed on the cell surface and is a component of GAGs such as chondroitin sulfate [38-40]. However, we did not observe CD44 gene expression in Jurkat cells, suggesting minimal

expression of chondroitin sulfate. We also observed expression of the glypican-1 gene, although its role in bacterial attachment to the Jurkat cells remains unknown. We therefore concluded that *C. pneumoniae* could infect lymphoid Jurkat cells, which poorly expressed PG-core proteins, and associated with minimal expressions of GAGs, implying that the presence of an attachment mechanism was independent of heparin.

Finally, we assessed co-localization of *C. pneumoniae* and heparin on the cellular surface of Jurkat cells immediately after infection. The presence of heparin on Jurkat cells was also compared with that on HEp-2 cells. Heparin staining with a single antibody indicated a strong surface expression of heparin on both epithelial cell types and also changes in fluorescence intensity between cells. Thus, microscopic analysis suggested that heparin expression on the epithelial cells used for this study were heterolytic and polarized. In contrast, the heparin expression on Jurkat cells was limited and co-localization between *C. pneumoniae* attachment and cellular surface heparin was not observed. This suggests that the *C. pneumoniae* mechanism of attachment to Jurkat cells is independent of heparin, the most well-known receptor for pathogen attachment to cells [17-22]. Since co-localization on positive control HEp-2 cells expressing heparin was only partially detected, we could not rule out that the detection limit of our fluorescence microscopy analysis system was not sufficient to detect week signals of co-localization. However, together these results indicate limited expression of GAGs, including heparin, in Jurkat cells and that heparin is unlikely to play a role in the attachment of *C. pneumoniae* to these cells, although it could not deny the attachment of *C. pneumoniae* to Jurkat cells via a few amount of heparin branching on glypican-1, only expressing on Jurkat cells.

There are intriguing evidences showing primary human $CD4^+$ lymphocytes, not expressing detectable level of heparin [38-40]. We therefore used the purified human $CD4^+$ lymphocytes for assessment of *C. pneumoniae* infection to lymphocytes independent of heparin. To prevent the activation of primary lymphocytes, a separation method with negative selection by depleting B cells, NK cells, monocytes, platelets, dendritic cells, $CD8^+$ T cells, granulocytes and erythrocytes, was chosen. The degree of refining of $CD4^+$ T cells was approximately 100 %, and no detectable level of heparin on the purified cells was also observed (data not shown). The inclusions observed into the purified lymphocytes were relatively small and ring-like structures, possibly associated with narrow space of the cells. Although we attempted to assess the number of infectious progenies in the infected lymphocytes, no increase of the bacterial numbers was observed (data not shown), indicating that persistent infection in the primary lymphocytes occurs, in contrast to Jurkat cells harboring the infectious progenies capable of secondary infection. The differences of bacterial growth between in Jurkat cells and primary cells remain unknown, but our pervious studies showing mouse and human lymphocyes as host cells for *C. pneumoniae* infection [14, 15] are also supporting successful infection to both Jurkat cells and $CD4^+$ T-lymphocytes in this study.

It has been well characterized that GAGs are required for binding of *C. pneumoniae* OmcB and GroEL1 molecules [21, 22], followed by successful infection. On the other hand, recent work regarding polymorphic membrane proteins (Pmps) interestingly indicated that yeast cells expressing Pmps adhered equally well to GAG-deficient CHO

cells and the control CHO K1 cells [41]. This report implies the presence of GAG-independent attachment mechanism on the interaction between *C. pneumoniae* and host cells, supporting our results in the present study. Although further study should be needed, it is possible that the major mechanism by which *C. pneumoniae* attached to lymphocytes might be independent of heparin, followed by successful infection.

Although it remains unknown the exact reason why *C. pneumoniae* purposely uses heparin-independent mechanism for attachment and entry to lymphocytes, there are some hints to solve this question, as below. Heparin independent attachment and host invasion has also been described for the *C. trachomatis* LGV invasive serotype causing a systemic disease, but not for any other serotypes [17-22]. This suggests that a heparin-independent attachment mechanism is useful for a pathogen to effectively spread from local lesions, such as the genital tract in this case, to other distinct lymphoid tissue, as observed in pelvic inflammatory disease [42]. Although further study is required to clarify why the *C. pneumoniae* attachment mechanism differs between cell types, this difference may contribute to the onset of inflammation, potentially associated with chronic disease such as atherosclerosis, as the bacteria spread from lung tissue to blood vessels.

4. Conclusions

In conclusion, our study demonstrated that *C. pneumoniae* attachment to Jurkat cells is unique as compared with that of HEp-2 cells and probably independent of heparin. These results further our understanding of the mechanisms that allow a pathogen to

evade a host's immune detection system and spread from a local lesion to a systemic lesion, such as in a blood vessel.

5. Materials and methods

5.1. Bacteria

C. pneumoniae TW183 strain was kindly provided by G. Byrne, University of Tennessee, Memphis, TN. Bacteria were propagated in the HEp-2 cell culture system as described previously [38]. In brief, the infected cells were harvested on day 3 and disrupted by freeze-thawing and ultrasonication. After centrifugation to remove cell debris, bacteria were concentrated by high-speed centrifugation. Bacterial pellets were resuspended in sucrose-phosphate-glutamic acid buffer (0.2 M sucrose, 3.8 mM KH_2PO_4, 6.7 mM Na_2HPO_4, 5 mM L-glutamic acid, pH 7.4) and then stored at –80°C for later use. The number of infectious *C. pneumoniae* was determined as inclusion forming units (IFUs) by counting chlamydial inclusions formed in HEp-2 cells as described below [38].

5.2. Cells

The epithelial cell line HEp-2 cells and lymphocyte cell line Jurkat cells were cultured at 37°C in 5 % CO_2 in DMEM medium and RPMI1640 medium respectively, each containing 10% heat-inactivated fetal calf serum and antibiotics (gentamicin 10 μg/ml; vancomycin 10 μg/ml; amphotericin B 1 μg/ml) (Sigma, St. Louis, MO). Human peripheral blood monocytes were isolated from whole blood provided by healthy volunteers, by density gradient centrifugation with Histopaque (Sigma). Primary human

$CD4^+$ lymphocytes were purified by the method with Dynabeads Untouched Human $CD4^+$ T cells kit (Invitrogen) according to the manufacture's protocol. The degree of refining of $CD4^+$ T cells was approximately 100 % by the immunofluorescence microscopic observation with fluorescein isothiocyanate (FITC)-conjugated monoclonal anti-human CD4 antibody (Becton-Dicknson). Informed consent with written was obtained from all volunteers in this study, and the study was approved by the ethics committee of Faculty of Health Sciences, Hokkaido University.

5.3. C. pneumoniae infection

The cells (HEp-2 cells, Jurkat cells, and primary human $CD4^+$ lymphocytes) were adjusted to a concentration of 5×10^5 cells/well and infected with bacteria at multiplicities of infection (MOI) of 1-200 either by static culture or by centrifugation (800×g) for 1 h at room temperature. After washing to remove non-infected bacteria with Hank's balanced solution (HBSS) (Sigma), infected and uninfected cells at a concentration of 5×10^5 cells/well were incubated for 3 days in the presence or absence of GAGs (500 μg/ml) (heparan sulfate, condroitin sulfate, hyaluronic acid) (Sigma). The cells were collected immediately after infection (3 h) and then daily for the entire culture period for infectious progeny assessment (IFU assay), inhibition assays with GAGs (immunofluorescence microscopy and flow cytometry), PG-related gene expression assessment using RT-PCR and evaluation of co-localization of the bacteria and heparin on the surface of cells and/or inclusion formation (immunofluorescence microscopy and/or transmission electron microscopy). Although the non-infected and infected epithelial HEp-2 cells were collected from culture dishes by trypsin (Sigma)

detachment, we confirmed that trypsin had no effect on cell viability and the effect on bacterial attachment rate was minimal (data not shown). We also confirmed that as compared the cell viability of Jurkat cells infected between with and without the bacteria, however, there was no difference of cell viability between the cells, during culture period (data not shown).

5.4. Assessment of inclusion formations

At 3 days after infection, the cells were collected for determination of morphology of chlamydial inclusions, as described previously [43]. In brief, after the cells were fixed on the slide with ethanol, the cells were stained with FITC-conjugated monoclonal anti-*Chlamydia* antibody specific to *Chlamydia* lipopolysaccharide (LPS) (with Evans Blue) (Denka Seiken Co. Ltd., Tokyo, Japan). The cells stained with specific antibodies were observed on viewing by conventional or confocal laser microscopy.

5.5. IFU assay

The number of infectious *C. pneumoniae* was determined using an IFU assay by counting chlamydial inclusions formed in HEp-2 cells using fluorescein isothiocyanate (FITC)-conjugated monoclonal anti-*Chlamydia* antibody specific to *Chlamydia* lipopolysaccharide (LPS) (with Evans Blue) (Denka Seiken Co. Ltd., Tokyo, Japan) [38].

5.6. Transmission electron microscopy

Transmission electron microscopy (TEM) was performed in accordance with a method

described previously [14]. In brief, bacteria in cultures were immersed in a fixative containing 3% glutaraldehyde in 0.1 M PBS pH 7.4, for 24 h at 4°C. After a brief wash with PBS, they were processed for alcohol dehydration and embedded in Epon 812. Ultrathin sections of cells were stained with lead citrate and uranium acetate before viewing by TEM (Hitachi H7100; Hitachi, Tokyo, Japan).

5.7. Assessment of bacterial attachment to cells

Bacterial attachment to cells was examined immediately after infection by immunofluorescence microscopy and flow cytometry using a FITC-conjugated monoclonal anti-*Chlamydia* antibody specific to *Chlamydia* LPS (without Evans Blue) (Progen Biotechniik, Deutschland, Germany). For analysis with immunofluorescence microscopy, the cells were washed in cold phosphate-buffered saline (PBS) containing 1% (w/v) bovine serum albumin (BSA) and then fixed in PBS containing 70% ethanol. The fixed cells were incubated with FITC-labeled *Chlamydia* LPS antibody. The percentage of the cells with attached bacteria was also estimated under immunofluorescence microscopy by counting at least 200 cells in three random fields for each sample. For analysis with flow cytometry, the cells were fixed using a kit, Cytofix/Cytoperm^{TM} kit (BD Biosciences, San Jose, CA) according to the manufacture protocol and then incubated with FITC-labeled *Chlamydia* LPS antibody. Ten thousand cells were analyzed using a EPICS-XL flow cytometer (Beckman Coulter, CA) immediately after labeling. The mean fluorescence intensity was obtained from the recorded data.

5.8. RT-PCR

Total RNA was extracted from cultures using an RNeasy Mini Kit (Qiagen, Valencia, CA) according to manufacturer's instructions. Extracted RNA was treated with DNase (DNA-free; Ambion, Austin, TX) to eliminate any contaminating DNA. PCR without RT was used confirm the absence of DNA. RNA (1 μg) was reverse transcribed using avian myeloblastosis virus reverse transcriptase with random primers in a commercial reaction mixture (Reverse Transcription System; Promega, Madison, WI). Synthesized cDNA was used for PCR amplification with primers specific for *syndecan-1* (sense, 5'-GAT GGC TCT GGG GAT GAC TC-3'; antisense, 5'-TGT TTG GTG GGC TTC TGG TAG-3') [44], *syndecan-2* (sense, 5'-GGG AGC TGA TGA GGA TGT AG-3'; antisense, 5'-CAC TGG ATG GTT TGC GTT CT-3') [44], *syndecan-4* (sense, 5'-CGA GAG ACT GAG GTC ATC GAC-3'; antisense, 5'-GCG GTA GAA CTC ATT GGT GG-3') [44], *betaglycan* (sense, 5'-CTG TCC ACC CGA CCT GAA AT-3'; antisense, 5'-CGT CAG GAG GCA CAC ACT TA-3') [44], *glypican-1* (sense, 5'-ATC ACC GAC AAG TTC TGG GGT TA-3'; antisense, 5'-CAT CTT CTC ACT GCA CAG TGT C-3') [44], *CD44* (sense, 5'-ATG GTT ATG TTT CCA ACG G-3'; antisense, 5'-GTG GAC TCA ACG GAG AGG-3') [45], *thrombomodulin* (sense, 5'-CTC ATA GGC ATC TCC ATC GCG-3'; antisense, 5'-CCG CGC ACT TGT ACT CCA TCT-3') [46], *C. pneumoniae 16S rRNA* (sense, 5'-GGA CCT TAG CTG GAC TTG ACA TGT-3'; antisense, 5'-CCA TGC AGC ACC TGT GTA TCT G-3') [47], and glyceraldehyde 3-phosphate dehydrogenase (*GAPDH*) (sense, 5'-AAC GGG AAG CTC ACT GGC ATG-3'; antisense, 5'-TCC ACC AAC CTG TTG CTG TAG-3') [44].

5.9. Heparin detection and co-localization with attached bacteria on the cell surface

Epithelial cells (HEp-2 cells and CHO K1 cells) were separately grown on a cover slip.

Immediately after infection, non-infected and infected cells were washed in cold PBS containing 5% (w/v) bovine serum albumin (BSA) and then fixed in PBS containing 1% (for single staining) or 3% (for dual staining) (w/v) paraformaldehyde. Fixed cells were incubated with FITC-labeled *Chlamydia* LPS antibody (without Evans Blue) (Progen) and/or unlabeled heparan sulfate antibody (Seikagaku, Tokyo, Japan) and then with Dylight^{TM} 549-labeled secondary antibody (American Qualex, CA). After staining, heparin was detected and assessed for co-localization with the bacteria using conventional and confocal fluorescence microscopy, respectively.

5.10. Statistical analysis

Statistical analysis was performed using an unpaired Student *t* test.

Acknowledgements

Kobayashi M and Ishida K contributed equally to this work. This study was supported in part by grants-in-aid for scientific research from KAKENHI, the Suhara Memorial Foundation, the Akiyama Foundation, and a research grant from the Institute for Fermentation, Osaka, Japan.

References

[1] Grayston JT. *Chlamydia pneumoniae*, strain TWAR. Chest 1989; 95: 664-9.

[2] Grayston JT, Wang SP, Kuo CC, Campbell LA. Current knowledge on *Chlamydia pneumoniae*, strain TWAR, an important cause of pneumonia and other acute respiratory diseases. Eur J Clin Microbiol Infect Dis 1989; 8: 191-202.

[3] Kauppinen M, Saikku P. Pneumonia due to *Chlamydia pneumoniae*: prevalence, clinical features, diagnosis, and treatment. Clin Infect Dis 1995; 21 Suppl 3: S244-52.

[4] Grayston JT. *Chlamydia pneumoniae* and atherosclerosis. Rev Med Interne 1996; 17 Suppl 1: S45-7.

[5] Hahn DL, Dodge RW, Golubjatnikov, R. Association of *Chlamydia pneumoniae* (strain TWAR) infection with wheezing, asthmatic bronchitis, and adult-onset asthma. JAMA 1991; 266: 225-30.

[6] Norton R, Schepetiuk S, Kok TW. *Chlamydia pneumoniae* pneumonia with endocarditis. Lancet 1995; 345: 1376-7.

[7] Saario R, Toivanen A. *Chlamydia pneumoniae* as a cause of reactive arthritis. Br J Rheumatol 1993; 32: 1112.

[8] Ieven MM, Hoymans VY. Involvement of *Chlamydia pneumoniae* in atherosclerosis: More evidence for lack of evidence. J Clin Microbiol 2005; 43: 19-24.

[9] Jonasson L, Holm J, Skalli O, Bondjers G, Hansson GK. Regional accumulations of T cells, macrophages, and smooth muscle cells in the human atherosclerotic plaque. Arteriosclerosis 1986; 6: 131-8.

[10] Sullivan GW, Sarembock IJ, Linden J. The role of inflammation in vascular diseases. J Leukoc Biol 2000; 67: 591-602.

[11] Matsumoto A, Higashi N, Tamura A. Electron microscope observation on the effects of polymixin B sulfate on cell walls of *Chlamydia psittaci*. J Bacteriol 1973 113: 357-364.

[12] Matsumoto A, Manire, GP. Electron microscopic observations on the fine structure of cell walls of *Chlamydia psittaci*. J. Bacteriol 1970 104: 1332-1337.

[13] Rockey DD, Matsumoto A. The chlamydial developmental cycles. 2000, Pages 403-425. In: Prokaryotic Development (Brun, Y.V., and Shimkets, L.L eds) ASM Press, Washington D.C.

[14] Haranaga S, Yamaguchi H, Friedman H, Izumi S, Yamamoto Y. *Chlamydia pneumoniae* infects and multiplies in lymphocytes in vitro. Infect Immun 2001: 69: 7753-9.

[15] Yamaguchi H, Haranaga S, Friedman H, Moor JA, Muffly KE, Yamamoto Y. A *Chlamydia pneumoniae* infection model using established human lymphocyte cell lines. FEMS Microbiol Lett 2002; 216: 229-234.

[16] Kaul R, Uphoff J, Wiedeman J, Yadlapalli S, Wenman WM. Detection of *Chlamydia pneumoniae* DNA in CD3+ lymphocytes from healthy blood donors and patients with coronary artery disease. Circulation 2000; 102: 2341-2346.

[17] Zhang JP, Stephens RS. Mechanism of *C. trachomatis* attachment to eukaryotic host cells. Cell; 1992 69: 861-869.

[18] Gutiérrez-Martín CB, Ojcius DM, Hsia R, Hellio R, Bavoil PM, Dautry-Varsat A. Heparin-mediated inhibition of *Chlamydia psittaci* adherence to HeLa cells. Microb Pathog 1997; 22: 47-57.

[19] Taraktchoglou M, Pacey AA, Turnbull JE, Eley A. Infectivity of *Chlamydia trachomatis* serovar LGV but not E is dependent on host cell heparan sulfate. Infect Immun. 2001; 69: 968-976.

[20] Wuppermann FN, Hegemann JH, Jantos CA. Heparan sulfate-like glycosaminoglycan is a cellular receptor for *Chlamydia pneumoniae*. J Infect Dis 2001; 184: 181-187.

[21] Moelleken K, Hegemann JH. The *Chlamydia* outer membrane protein OmcB is

required for adhesion and exhibits biovar-specific differences in glycosaminoglycan binding. Mol Microbiol 2008; 67: 403-419.

[22] Wuppermann FN, Mölleken K, Julien M, Jantos CA, Hegemann JH. *Chlamydia pneumoniae* GroEL1 protein is cell surface associated and required for infection of HEp-2 cells. J Bacteriol. 2008; 190: 3757-3767.

[23] Kjellen L, Lindahl U. Proteoglycans: structures and interactions. Annu Rev Biochem 1991; 60: 443–475.

[24] Rostand KS, Esko JD. Microbial adherence to and invasion through proteoglycans. Infect Immun 1997; 65: 1-8.

[25] Jones KS, Petrow-Sadowski C, Bertolette DC, Huang Y, Ruscetti FW. Heparan sulfate proteoglycans mediate attachment and entry of human T-cell leukemia virus type 1 virions into $CD4^+$ T cells. J Virol 2005; 79: 12692-12702.

[26] Clasper S, Vekemans S, Fiore M, Plebanski M, Wordsworth P, David G, Jackson DG. Inducible expression of the cell surface heparan sulfate proteoglycan syndecan-2 (fibroglycan) on human activated macrophages can regulate fibroblast growth factor action. J Biol Chem 1999; 274: 24113-24123.

[27] Ibrahim J, Griffin P, Coombe DR, Rider CC, James W. Cell-surface heparan sulfate facilitates human immunodeficiency virus Type 1 entry into some cell lines but not

primary lymphocytes. Virus Res 1999; 60: 159-169.

[28] Saphire AC, Bobardt MD, Zhang Z, David G, Gallay PA. Syndecans serve as attachment receptors for human immunodeficiency virus type 1 on macrophages. J Virol 2001; 75: 9187-9200.

[29] Sutton RE, Littman DR. Broad host range of human T-cell leukemia virus type 1 demonstrated with an improved pseudotyping system. J Virol 1993; 70: 7322-7326.

[30] Yamaguchi H, Matsuo J, Sugimoto S, Utsumi M, Yamamoto Y. Inhibition of lymphocyte CD3 expression by *Chlamydophila pneumoniae* infection. Microb Pathog 2008; 45: 290-296.

[31] Hirai I, Utsumi M, Yamaguchi H, Yamamoto Y. *Chlamydia pneumoniae* infection suppresses Staphylococcus enterotoxin B-induced proliferation associated with down-expression of CD25 in lymphocytes. Can J Microbiol 2010; 56: 289-294.

[32] Dosch HM, White D, Grant C. Reconstitution of nude mouse T cell function in vivo: IL 2-independent effect of human T cells. J Immunol 1985; 134:336-342.

[33] Scidmore MA, Fischer ER, Hackstadt T. Sphingolipids and glycoproteins are differentially trafficked to the *Chlamydia trachomatis* inclusion. J Cell Biol 1996; 134: 363-374.

[34] Robertson DK, Gu L, Rowe RK, Beatty WL. Inclusion biogenesis and reactivation of persistent *Chlamydia trachomatis* requires host cell sphingolipid biosynthesis. PLoS Pathog 2009; 5: e1000664.

[35] Menozzi FD, Mutombo R, Renauld G, Gantiez C, Hannah JH, Leininger E, Brennan MJ, Locht C. Heparin-inhibitable lectin activity of the filamentous hemagglutinin adhesin of *Bordetella pertussis*. Infect Immun 1994; 62: 769-778.

[36] Noel GJ, Love DC, Mosser DM. High-molecular-weight proteins of nontypeable Haemophilus influenzae mediate bacterial adhesion to cellular proteoglycans. Infect Immun 1994; 62: 4028-4033.

[37] Van Putten JP, Paul SM. Binding of syndecan-like cell surface proteoglycan receptors is required for *Neisseria gonorrhoeae* entry into human mucosal cells. EMBO J 1995; 14: 2144-2154.

[38] Wegrowski Y, Milard AL, Kotlarz G, Toulmonde E, Maquart FX, Bernard J. Cell surface proteoglycan expression during maturation of human monocytes-derived dendritic cells and macrophages. Clin Exp Immunol 2006; 144: 485-493.

[39] Rostand KS, Esko JD. Microbial adherence to and invasion through proteoglycans. Infect Immun 1997; 65:1-8.

[40] Schofield KP, Gallagher JT, David G. Biochem J. Expression of proteoglycan core

proteins in human bone marrow stroma. 1999; 343 (Pt 3): 663-668.

[41] Mölleken K, Schmidt E, Hegemann JH. Members of the Pmp protein family of *Chlamydia pneumoniae* mediate adhesion to human cells via short repetitive peptide motifs. Mol Microbiol 2010; 78: 1004-1017.

[42] Mårdh PA. Tubal factor infertility, with special regard to chlamydial salpingitis. Curr Opin Infect Dis 2004; 17:49-52.

[43] Roblin PM, Dumornay W, Hammerschlag MR. Use of HEp-2 cells for improved isolation and passage of *Chlamydia pneumoniae*. J Clin Microbiol 1992; 30:1968-1971.

[44] Gnoatto N, Lotufo RF, Matsuda M, Penna V, Marquezini MV. Expression of cell-surface heparan sulfate proteoglycans in human cyclosporin-induced gingival overgrowth. J Periodontal Res 2007; 42: 553-558.

[45] Virok D, Loboda A, Kari L, Nebozhyn M, Chang C, Nichols C, Endresz V, Gonczol E, Berencsi K, Showe MK, Showe LC. Infection of U937 monocytic cells with *Chlamydia pneumoniae* induces extensive changes in host cell gene expression. J Infect Dis 2003; 188: 1310-1321.

[46] Dobra K, Andäng M, Syrokou A, Karamanos NK, Hjerpe A. Differentiation of mesothelioma cells is influenced by the expression of proteoglycans. Exp Cell Res 2000; 258: 12-22.

[47] Madico G, Quinn TC, Boman J, Gaydos CA. Touchdown enzyme time release-PCR for detection and identification of *Chlamydia trachomatis*, *C. pneumoniae*, and *C. psittaci* using the 16S and 16S-23S spacer rRNA genes. J Clin Microbiol 2000; 38: 1085-1093.

Legends to figures

Fig. 1. Representative TEM images showing the *C. pneumoniae* attachment and inclusion formation into Jurkat cells. (A) The inclusion formation of *C. pneumoniae* in HEp-2 cells as a control. Scale, 2μm. (B) Representative TEM images showing the attachment of *C. pneumoniae* to Jurkat cells. Arrowhead shows attachment of *C. pneumoniae* EB to a cell. Scale, 500 nm. (C) Square in the image (B) is enlarged. Parenthesis shows firm bacterial attachment to the Jurkat cell with bundle-like fibers (Arrows). (D) The inclusion formation of *C. pneumoniae* in Jurkat cells. Scale, 500nm.

Fig. 2. One-step growth curves for *C. pneumoniae* in HEp-2 cells and Jurkat cells. (A, C) Both cells were infected with bacteria at MOI of 1 either by static culture (A) or by centrifugation (C) for 1 h at room temperature (See the Materials and methods in text). The data shown represent the mean ± standard deviation (error bars). *p< 0.05 versus the value at immediately after infection (0 days). The squares in panel A and C indicate the data re-plotted to the attachment rates for panel B and D, respectively. (B, D) Attachment rates of *C. pneumoniae* to both cells shown as relative number of bacteria. The data shown represent the mean + standard deviation (error bars). *p< 0.05 versus the value of HEp-2 cells.

Fig. 3. Effect of GAGs on *C. pneumoniae* attachment to cells. Cells were infected with bacteria in the presence or absence of GAGs (heparan sulfate, condroitin sulfate,

hyaluronic acid) and at immediately (approximately 30 min) after infection the number of infected cells was determined using immunofluorescence microscopy (A) and flow cytometry. (B). HEp-2 cells and Jurkat cells were statically infected with bacteria at MOI of 50 and 200, respectively, for 1 h at room temperature (See the Materials and Methods in text). Data represent the mean + standard deviation (error bars) (A) and the mean ± standard deviation (B). *$p< 0.05$ versus the values of the infected cells without GAGs.

Fig. 4. Comparison of PG-core protein encoding gene expressions with regulating GAGs in HEp-2 cells and Jurkat cells. HEp-2 cells and Jurkat cells were statically infected with bacteria at a MOI of 1 and 50, respectively, for 1 h at room temperature (See the Materials and methods in text).

Fig. 5. Assessment of *C. pneumoniae* and heparin co-localization on the cell surface. (A)(B) Representative single-fluorescence staining images showing heparin expression on the cell [HEp-2 cells (A) and Jurkat cells (B)]. Green dots show heparin expression. The detection of heparin was assessed using conventional fluorescence microscopy. (C)(D) Representative double-fluorescence staining images showing the co-localization of *C. pneumoniae* and heparin on the HEp-2 cells (C) and the Jurkat cells (D). Both cells were statically infected with bacteria at MOI of 100 for 1 h at room temperature (See the Materials and Methods in text). Red and green dots show heparin expression and *C. pneumoniae* attachment to the cells, respectively. Orange dots also show the

co-localization of *C. pneumoniae* and heparin on the cells (arrows). Co-localization of heparin with the bacteria was assessed using confocal fluorescence microscopy.

Fig. 6. Attachment and specific inclusion formation of *C. pneumoniae* into purified human $CD4^+$ T lymphocytes. The cells were statically infected with bacteria at MOI of 100 for 1 h at room temperature (See the Materials and Methods in text). At immediately (approximately 30 min) or 3 days after infection, the cells were fixed and then incubated with FITC-labeled *Chlamydia* LPS antibody with (C-E) or without Evans blue (A, B). The attachment and inclusion formation were estimated under the observation with conventional (A, B) and confocal laser immunofluorescence microscopy (C-E). (A) Specific-inclusion formations of *C. pneumoniae* in purified human $CD4^+$ T lymphocytes under the observation with conventional immunofluorescence microscopy. Magnification, × 400. Squares (A-1 to A-5) in the image (A) are enlarged, respectively. Green, *C. pneumoniae*-specific inclusions. (B)(C) Negative control, uninfected $CD4^+$ T lymphocyte. (D) Attachment of *C. pneumoniae* to purified human $CD4^+$ T lymphocytes at immediately after infection under the observation with confocal laser immunofluorescence microscopy. Arrowhead shows attachment of *C. pneumoniae* particle on the cell surface. Green, *C. pneumoniae* particles. Red (Evans blue), $CD4^+$ T lymphocytes. (E) Specific-inclusion formation of *C. pneumoniae* in purified human $CD4^+$ T lymphocytes under the observation with confocal laser immunofluorescence microscopy (at 3 days after infection). The Z-axis image shows that cross-pointing small inclusion is formed inside the cell. Arrow shows *C. pneumoniae*-specific inclusion. Yellow (inside cell) and Green (remaining bacteria

outside cell), *C. pneumonia*-specific inclusion. Red (Evans blue), $CD4^+$ T lymphocytes.

Fig. 1

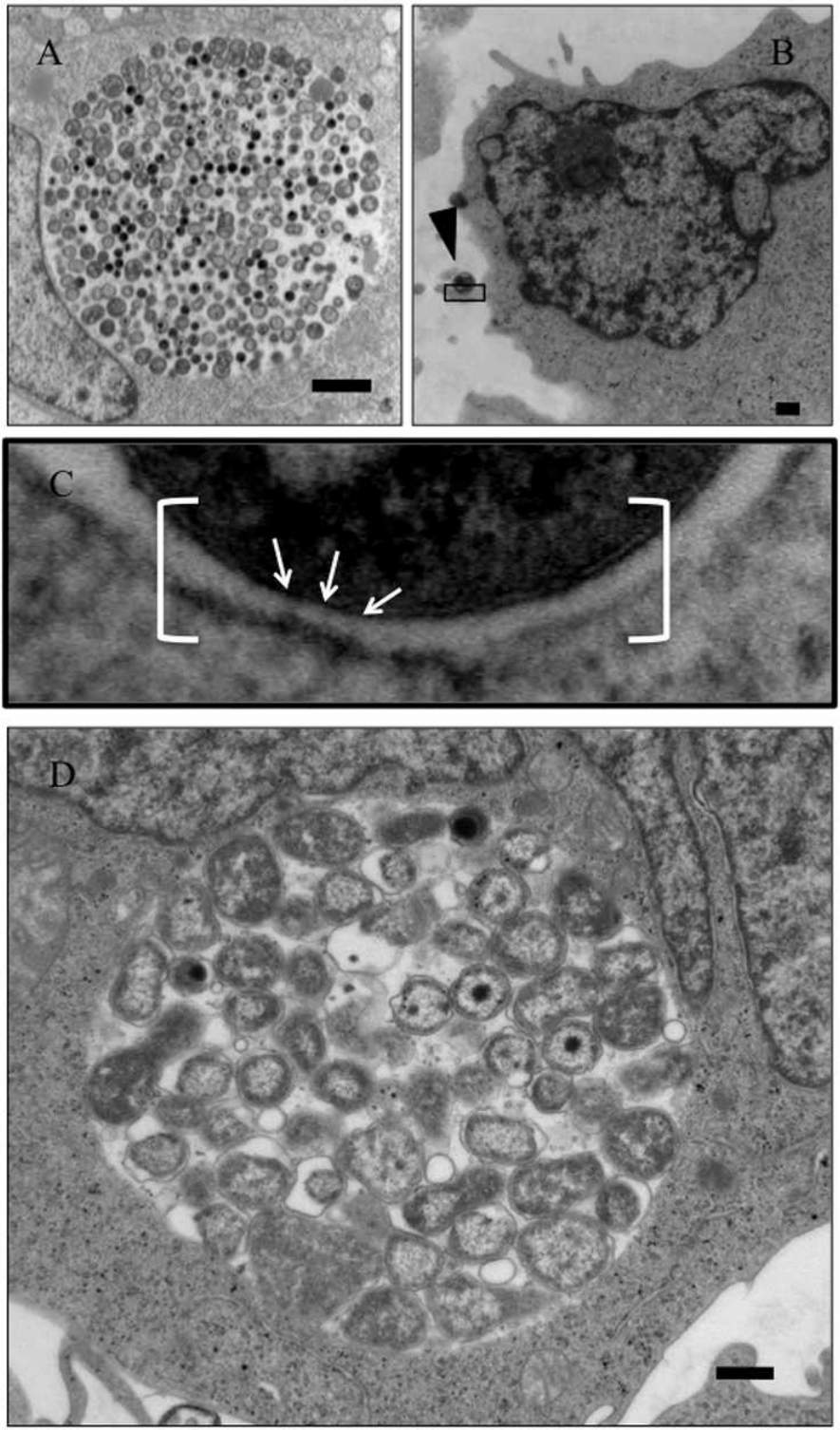

Fig. 2

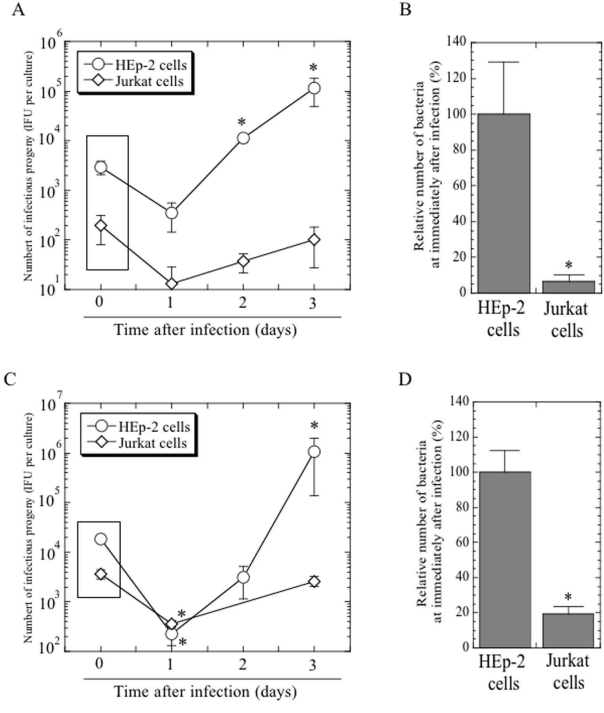
A
B
C
D
HEp-2 cells
Jurkat cells
Numbert of infectious progeny (IFU per culture)
Time after infection (days)
Relative number of bacteria at immediately after infection (%)
HEp-2 cells
Jurkat cells

Fig. 3

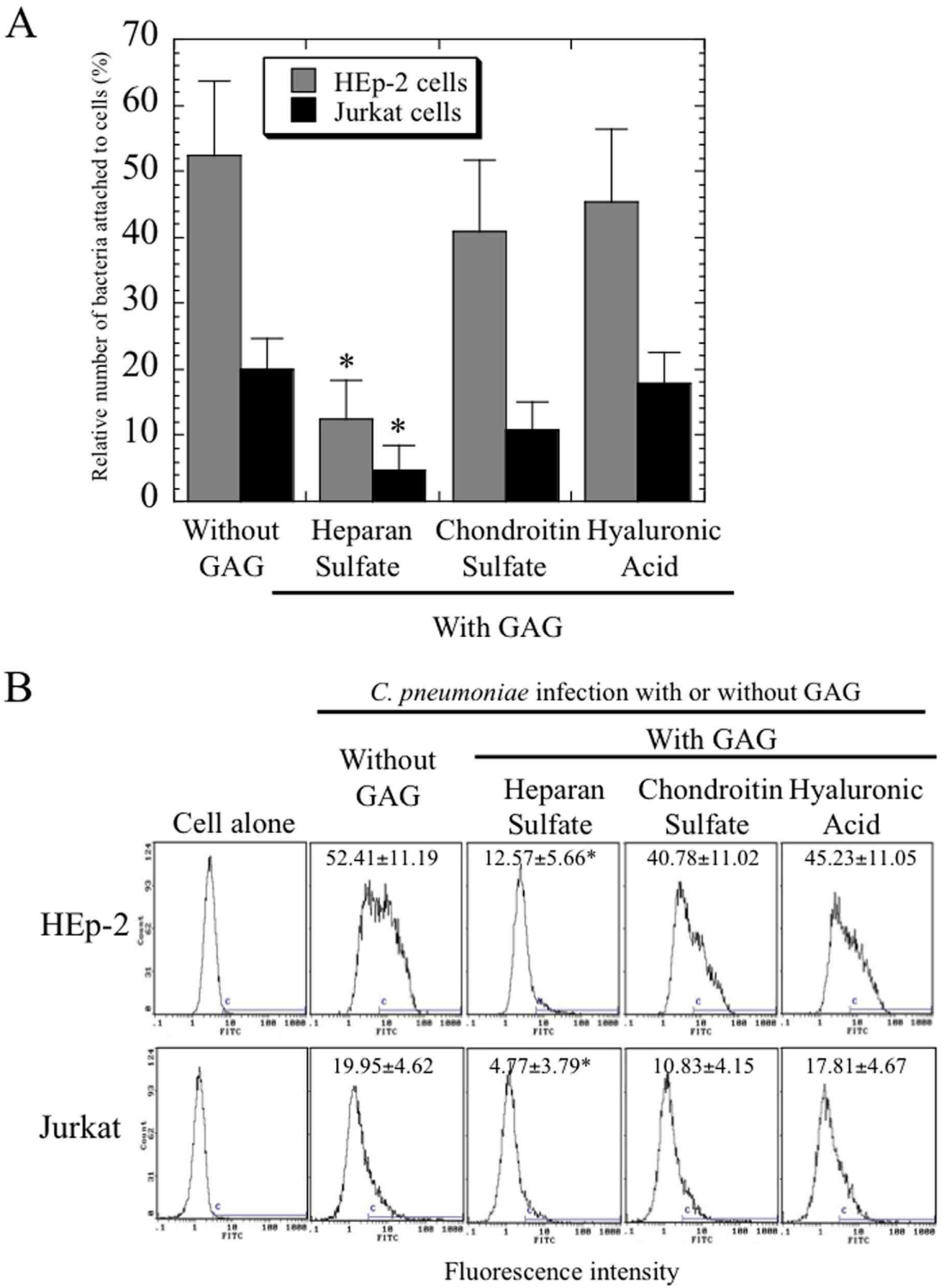
A
70
60
50
40
30
20
10
0
Relative number of bacteria attached to cells (%)
HEp-2 cells
Jurkat cells
*
*
Without GAG
Heparan Sulfate
Chondroitin Sulfate
Hyaluronic Acid
With GAG
B
C. pneumoniae infection with or without GAG
Without GAG
With GAG
Cell alone
Heparan Sulfate
Chondroitin Sulfate
Hyaluronic Acid
HEp-2
52.41±11.19
12.57±5.66*
40.78±11.02
45.23±11.05
Jurkat
19.95±4.62
4.77±3.79*
10.83±4.15
17.81±4.67
Count
FITC
Fluorescence intensity

Fig. 4

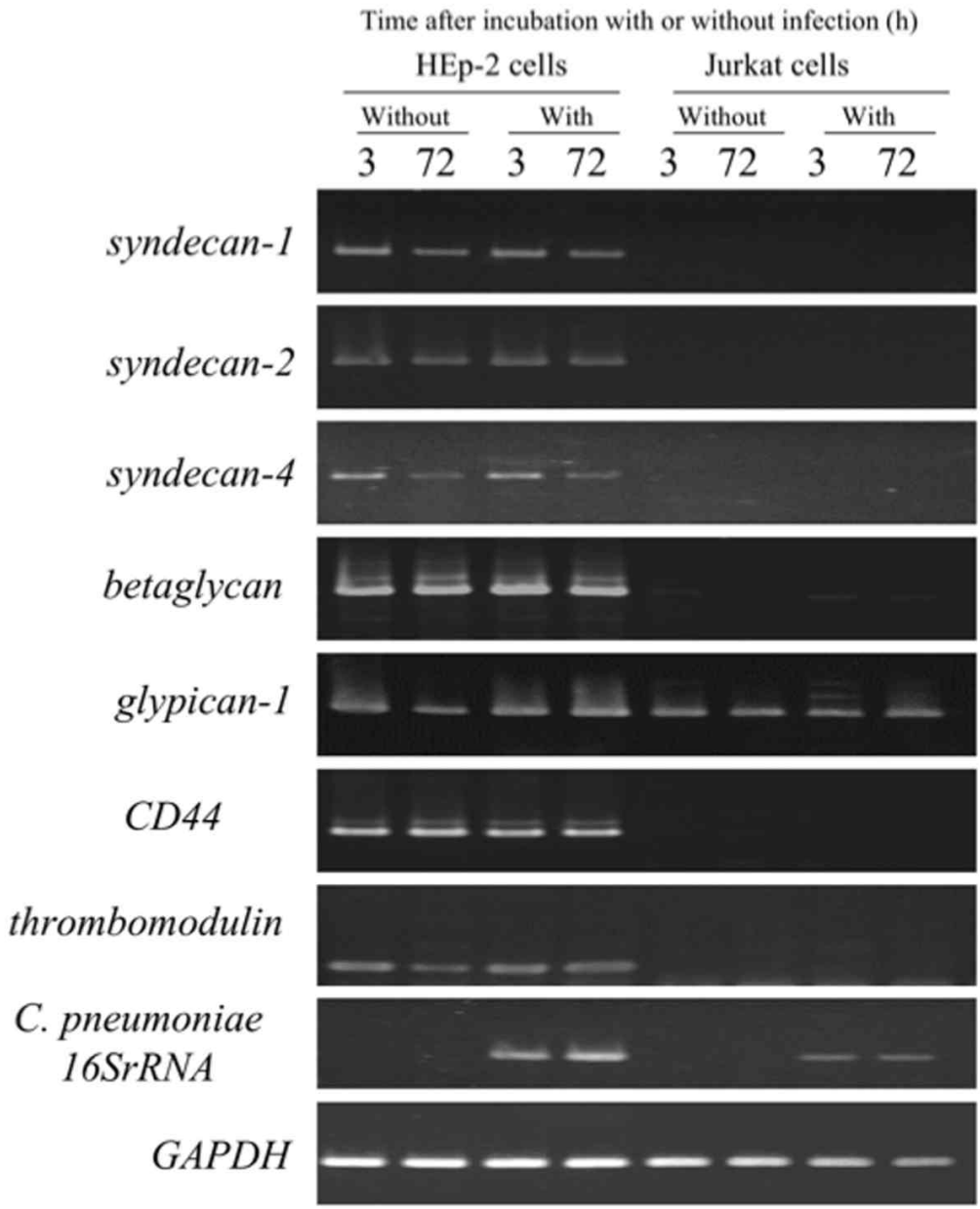
Time after incubation with or without infection (h)
HEp-2 cells
Jurkat cells
Without
With
Without
With
3
72
3
72
3
72
3
72
syndecan-1
syndecan-2
syndecan-4
betaglycan
glypican-1
CD44
thrombomodulin
C. pneumoniae 16SrRNA
GAPDH

Fig. 5

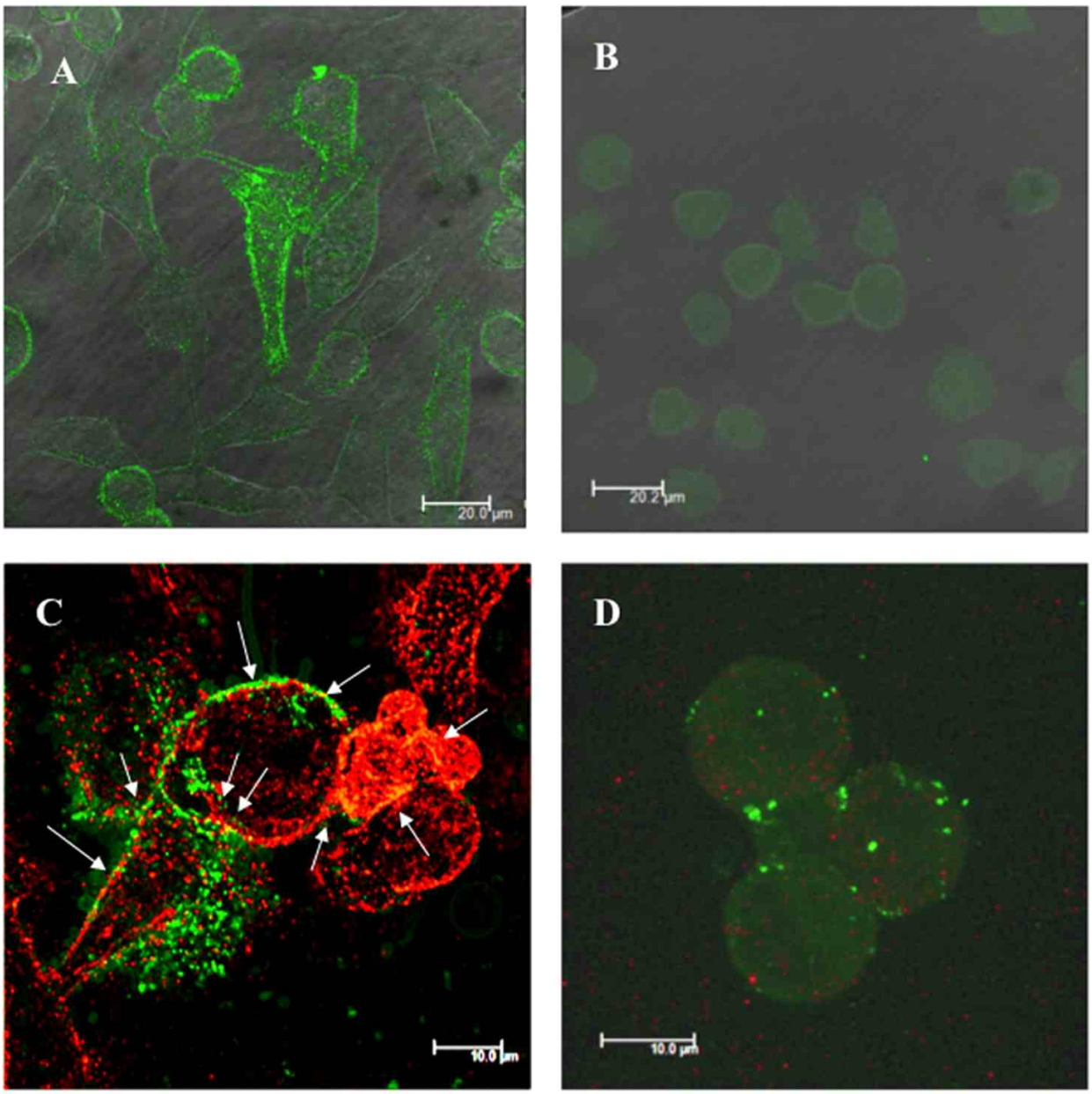

Fig. 6